Supplement of Hydrol. Earth Syst. Sci., 25, 41–61, 2021
https://doi.org/10.5194/hess-25-41-2021-supplement

Hydrology and Earth System Sciences
Open Access
EGU

Supplement of

Developing a hydrological monitoring and sub-seasonal to seasonal forecasting system for South and Southeast Asian river basins

Yifan Zhou et al.

Correspondence to: Benjamin F. Zaitchik (zaitchik@jhu.edu)

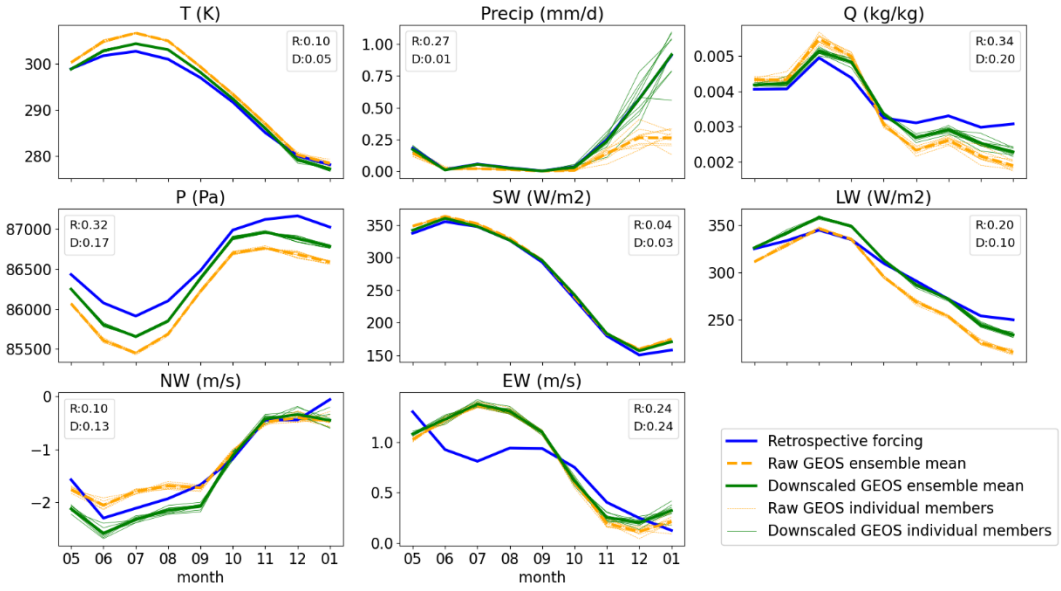

Figure S1: Comparison of Air temperature (T), precipitation (Precip), specific humidity (Q), surface pressure (P), solar radiation (SW), longwave radiation (LW), north-south wind speed (NW), east-west wind speed (EW) among Retrospective, raw GEOS-S2S-V1 and downscaled GEOS-S2S-V1 meteorological forcing in the Helmand basin. The root mean squared error normalized by the range of the retrospective meteorological forcing (NRMSE) is shown as the values in each subplot. R denotes the NRMSE between raw GEOS-S2S-V1 and retrospective forcing and D denotes the NRMSE between downscaled GEOS-S2S-V1 and retrospective forcing.

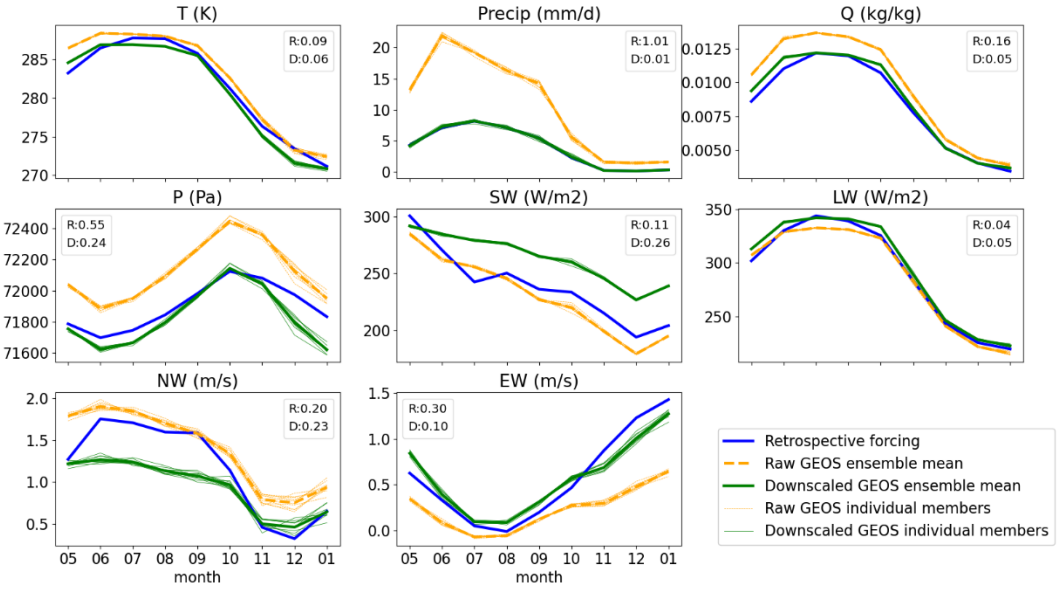

20 **Figure S2: The same as Fig. S1 but in the Brahmaputra basin.**

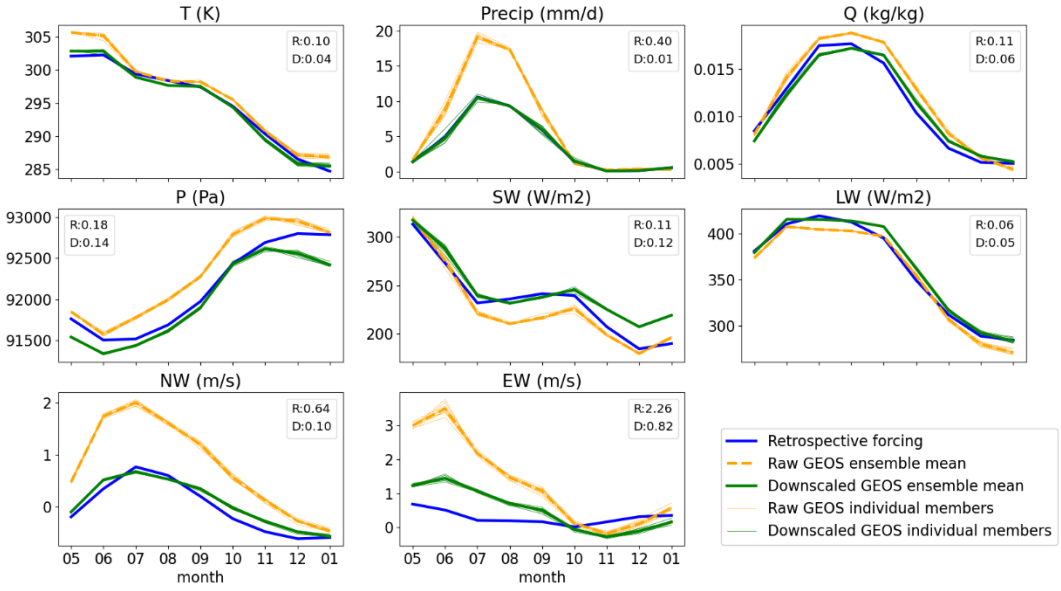

Figure S3: The same as Fig. S1 but in the Ganges basin

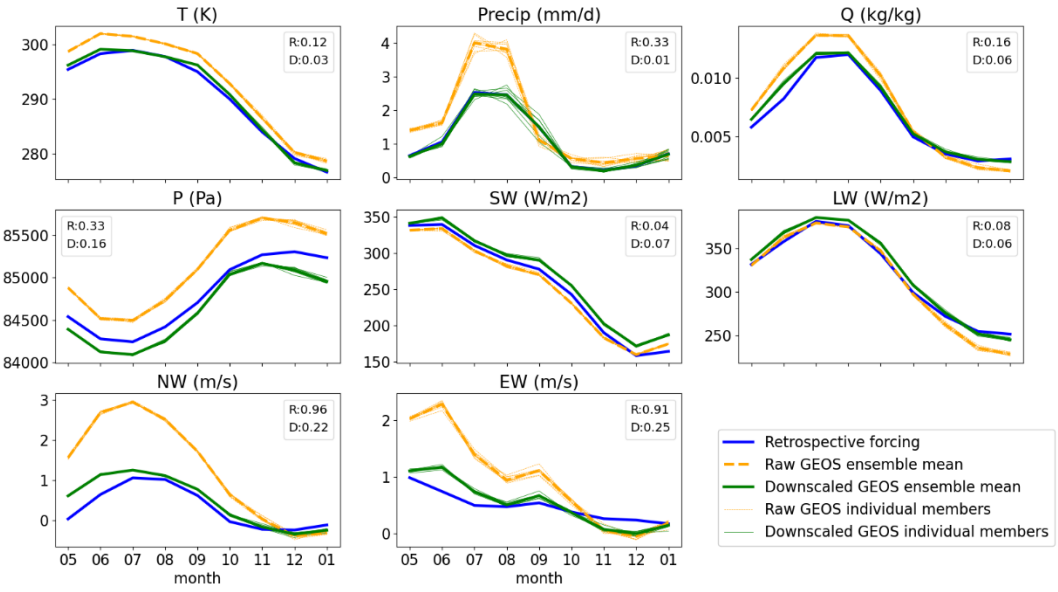

Figure S4: The same as Fig. S1 but in the Indus basin

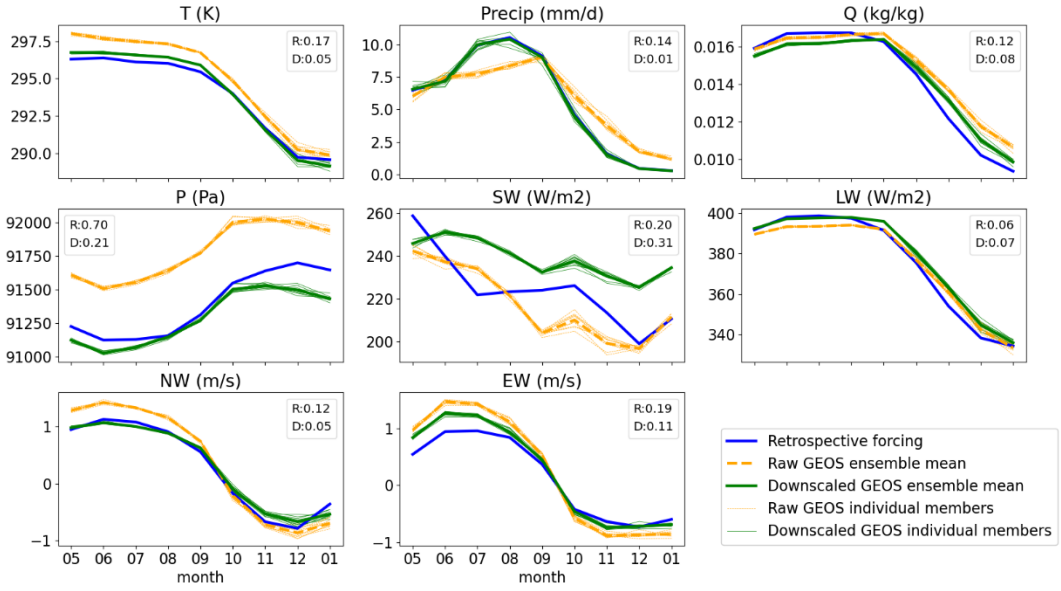

Figure S5: The same as Fig. S1 but in the Mekong basin

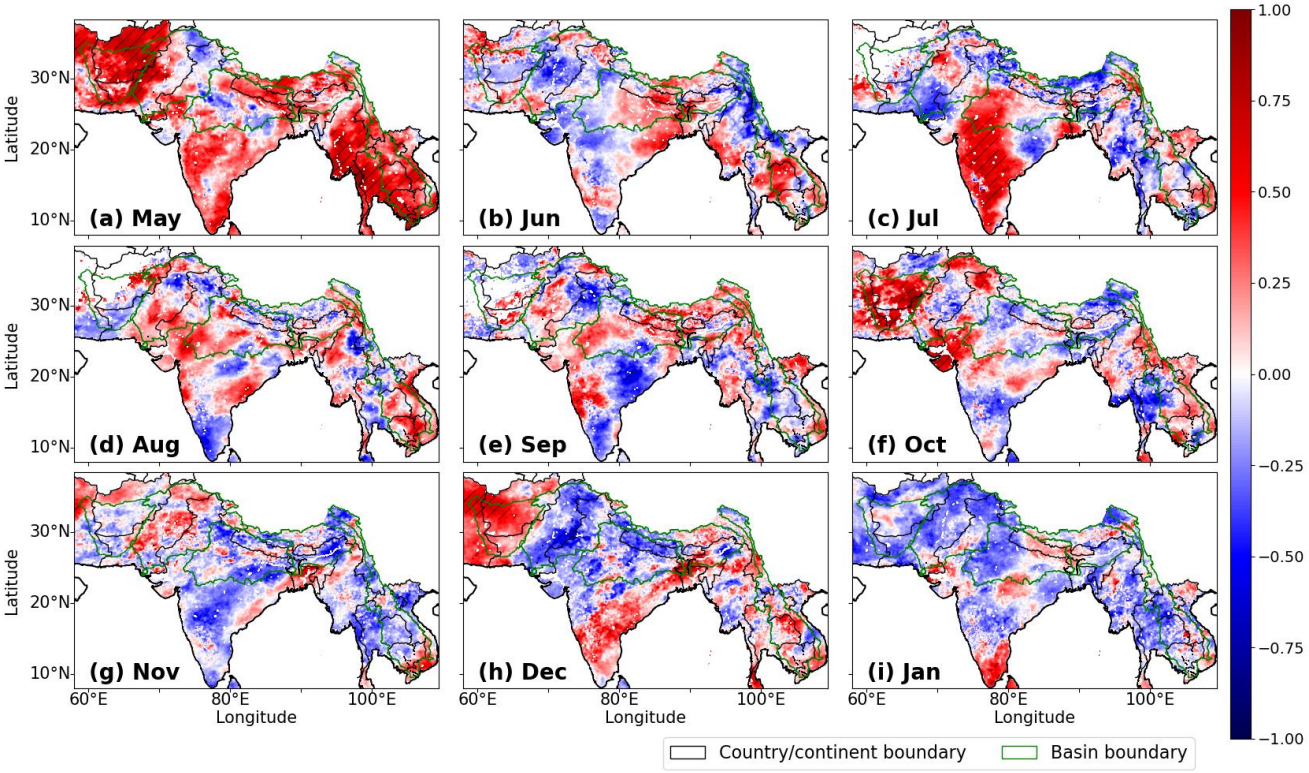

Figure S6: Interannual correlation of precipitation between retrospective simulations (i.e., CHIRPS) and hindcasting simulations (i.e., downscaled GEOS-S2S-V1 precipitation) which is computed using precipitation data from year 2000 to 2017 in months May (1-month lead time) to January (9-month lead time) (subplot (a) to subplot (i)). The hatches denote the areas with statistically significant correlation at 0.95 confidence level.

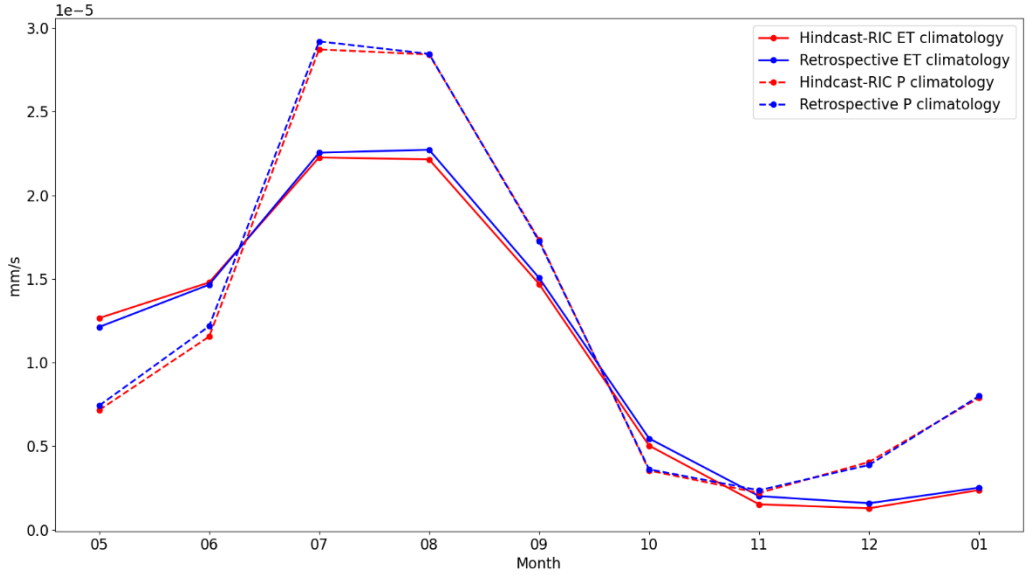

Figure S7. The climatological monthly precipitation and evapotranspiration (ET) in the Indus basin from retrospective and hindcast-RIC simulations.

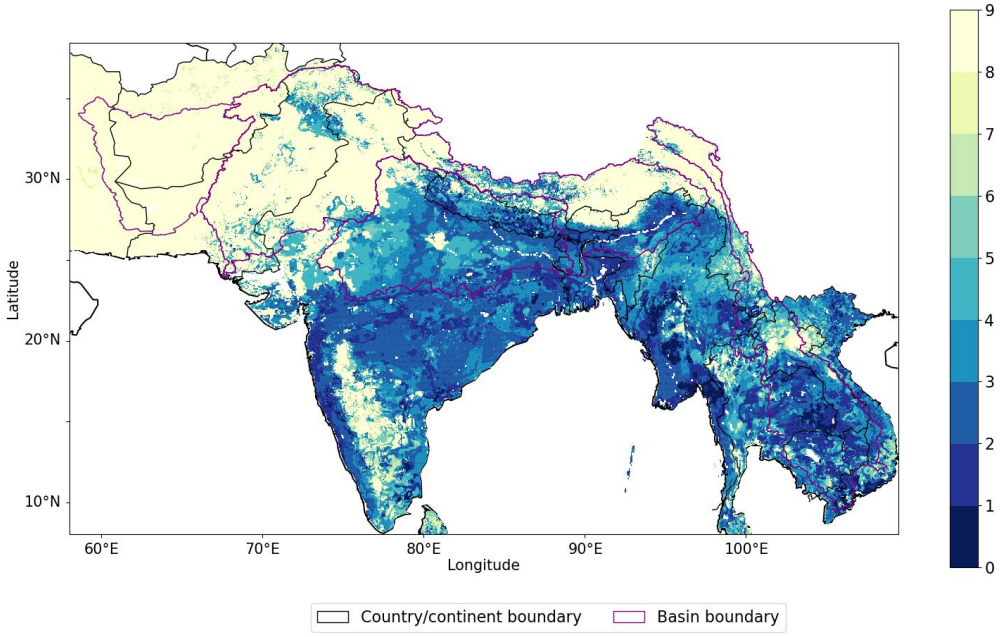

45

Figure S8: The largest lead month when the difference of RZSM forecast skills between hindcast-RIC and hindcast-CIC against retrospective simulations still remains statistically significant.

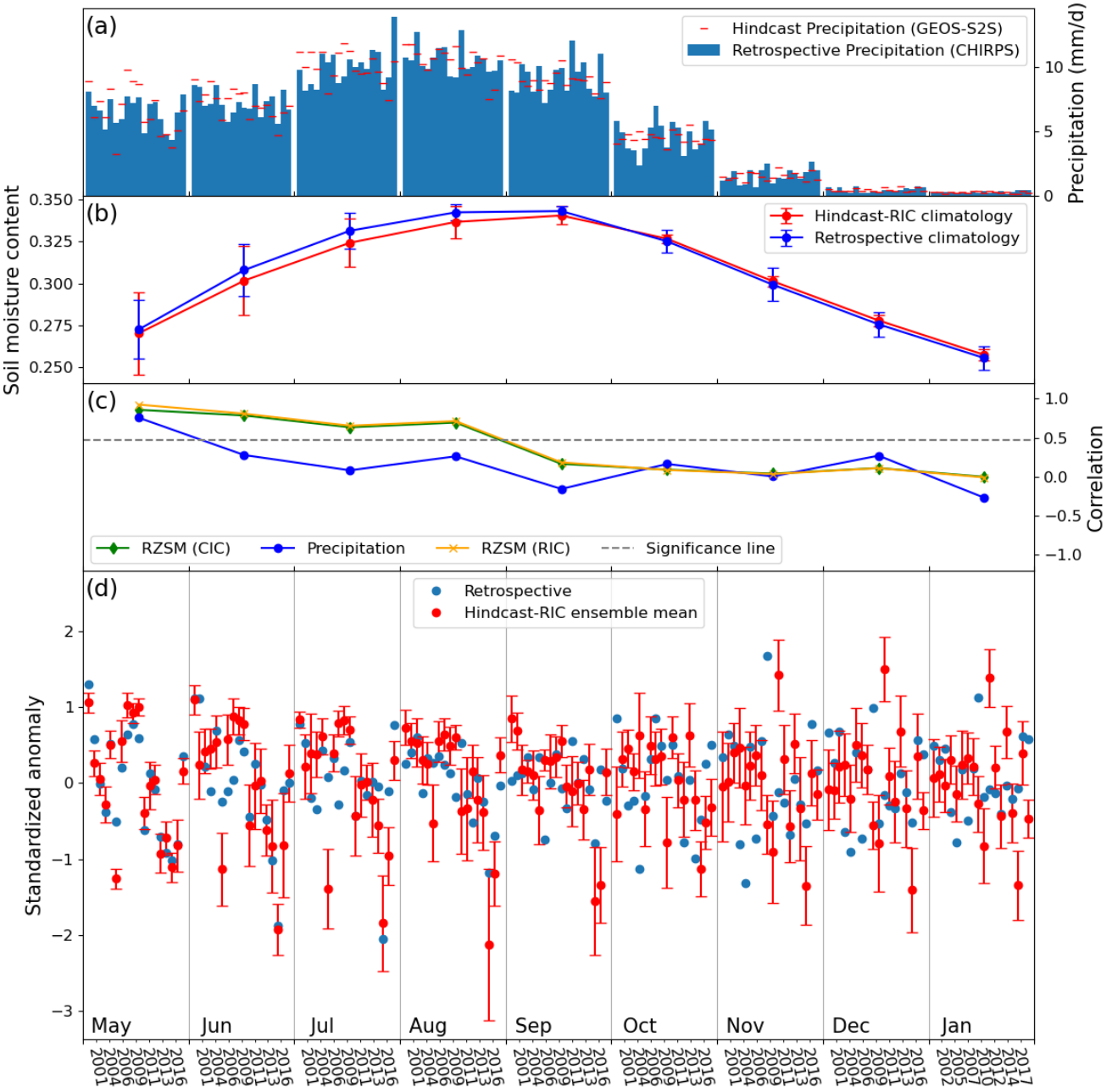

Figure S9: Comparison between retrospective simulations and hindcast simulations in the Mekong basin of (a) monthly time series of precipitation, (b) monthly climatology of root zone soil moisture (RZSM), (c) inter-annual correlations of basin-averaged RZSM standardized anomaly and precipitation, and (d) monthly standardized anomaly of RZSM (the red error bars represent for the standard deviation of separate hindcast ensemble members). Please note that the time axis for monthly time series are rearranged so that the data for the same month is grouped.

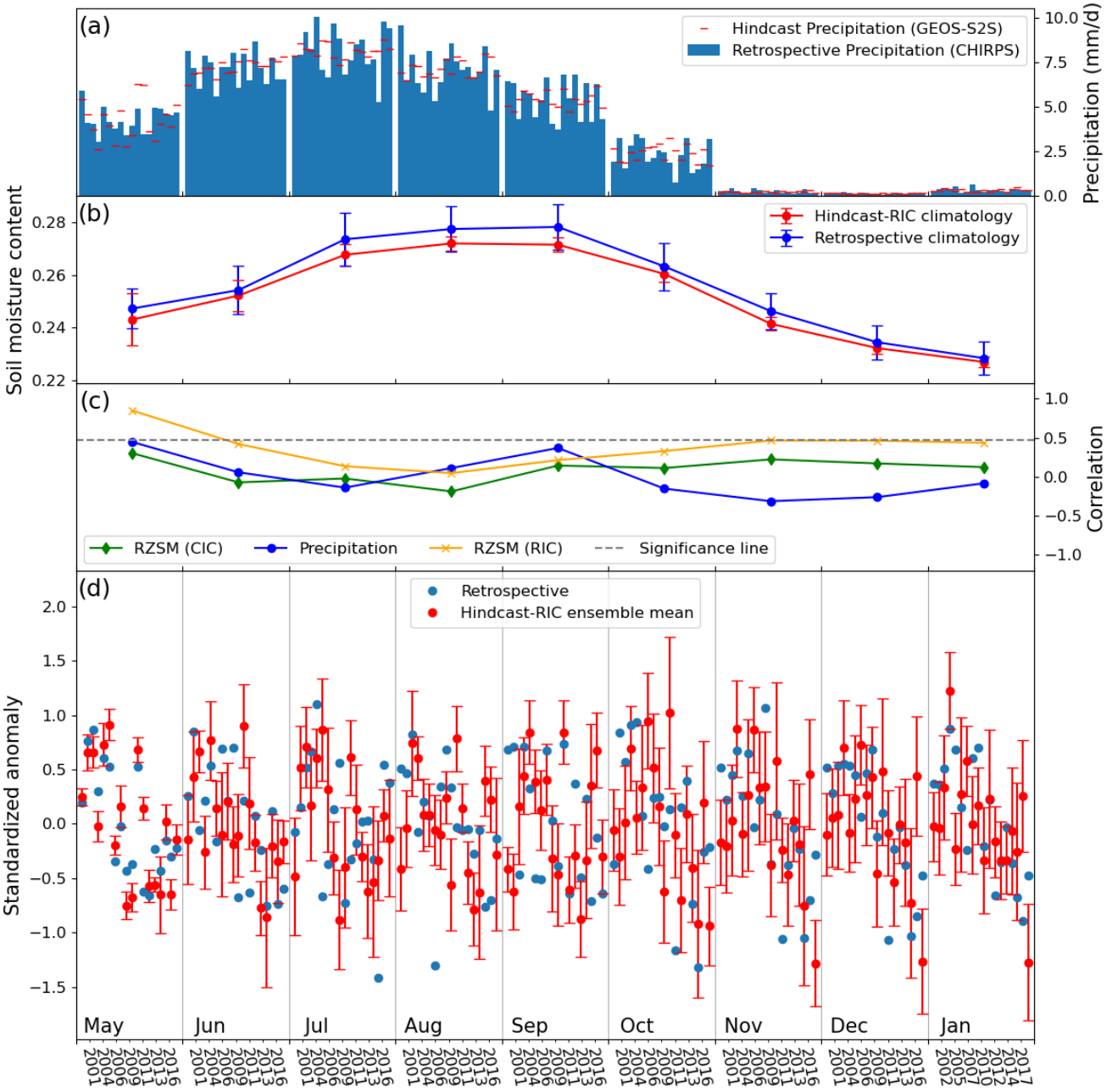

Figure S10: Same as Fig. S9, but for the Brahmaputra basin.

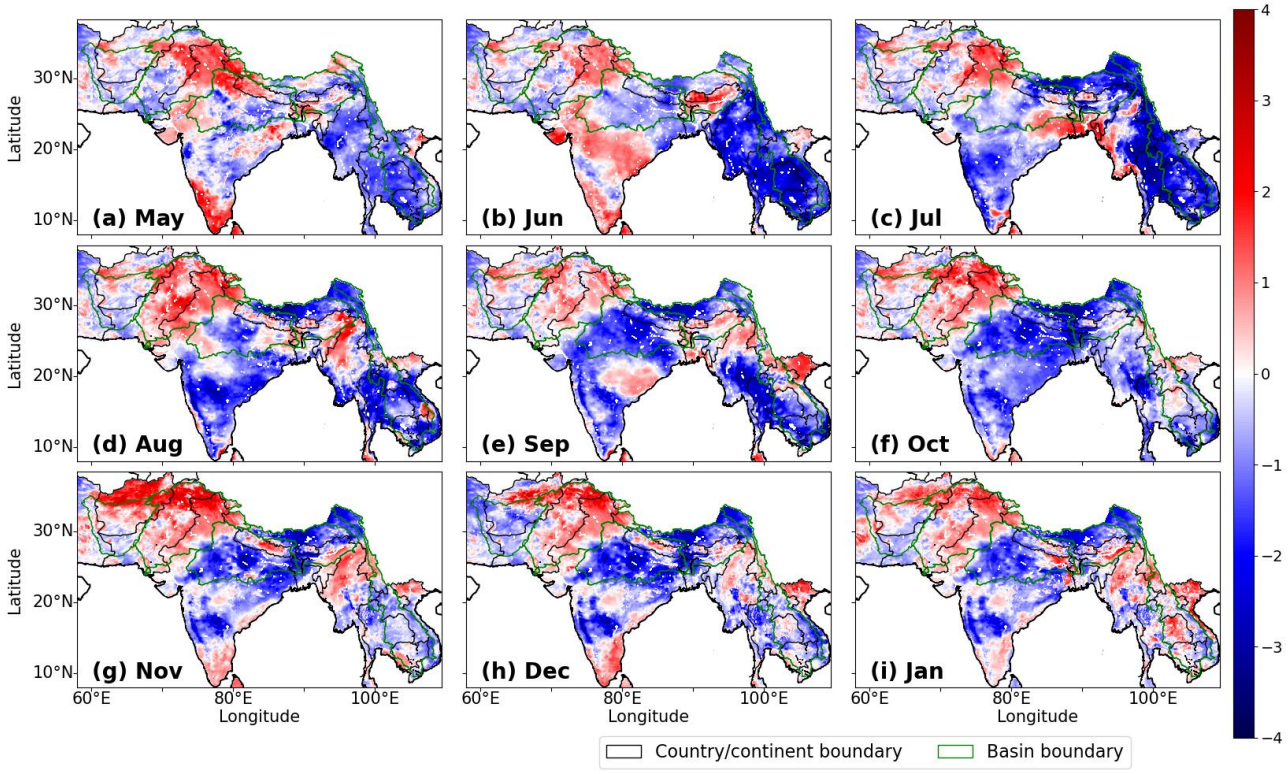

Figure S11. The spatial distribution of monthly RZSM standardized anomaly for 2015 South and Southeast Asia drought calculated from the retrospective simulation

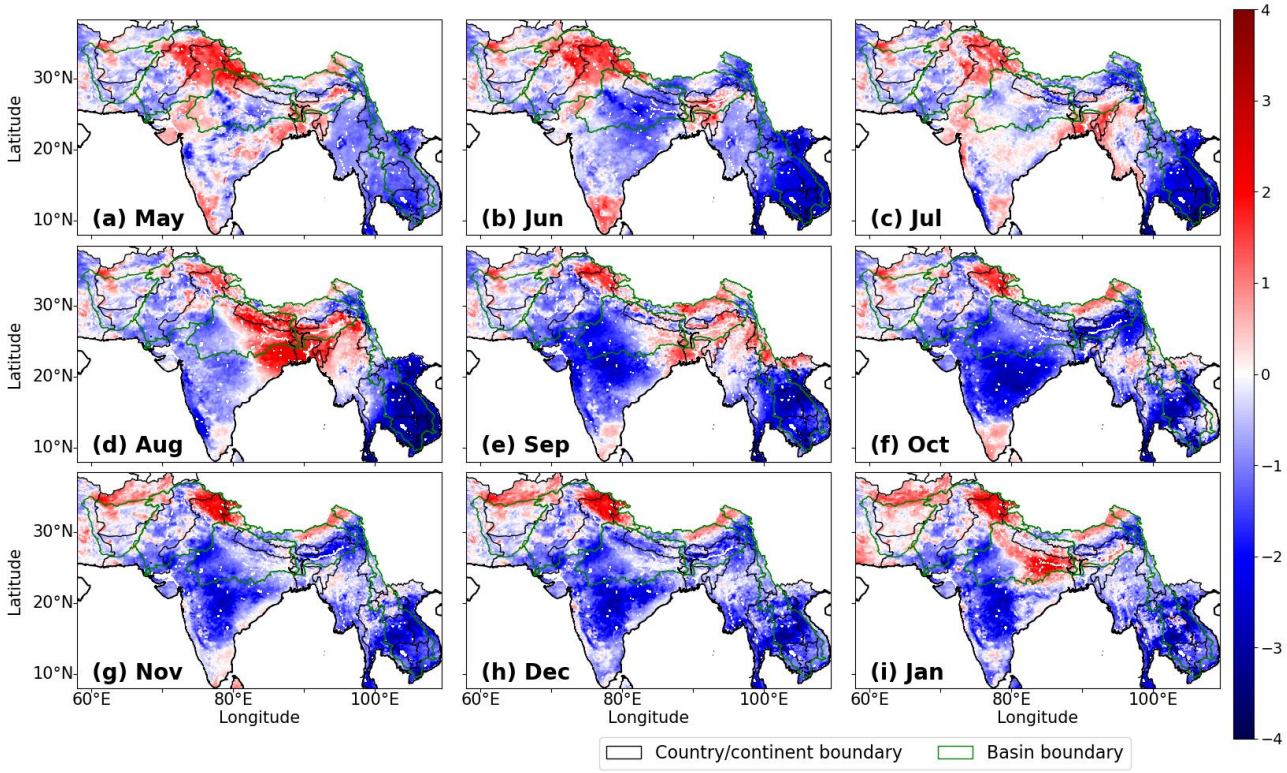

Figure S12. The same as Fig. S11 but calculated from ensemble mean of the hindcast-RIC simulation

70

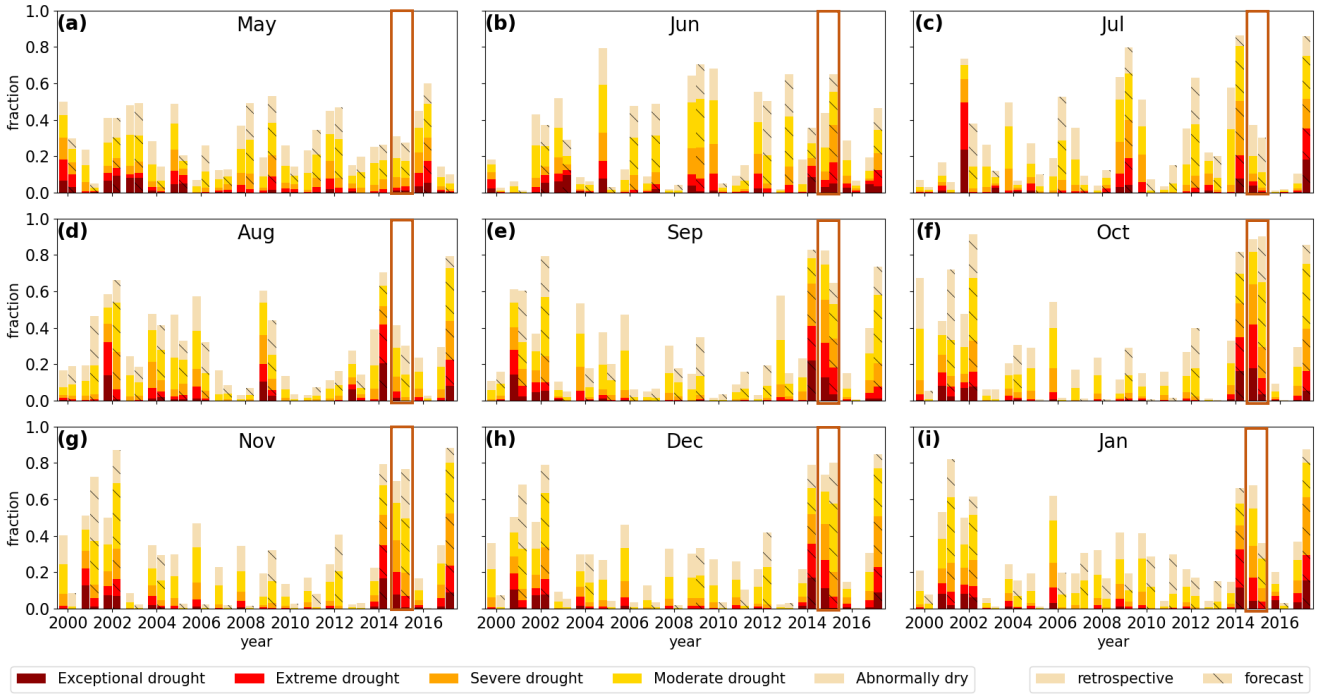

Figure S13: Fractions of areas of different drought categories in Ganges basin calculated using RZSM data from retrospective and hindcast-RIC simulations from (a) May to (i) January.

75

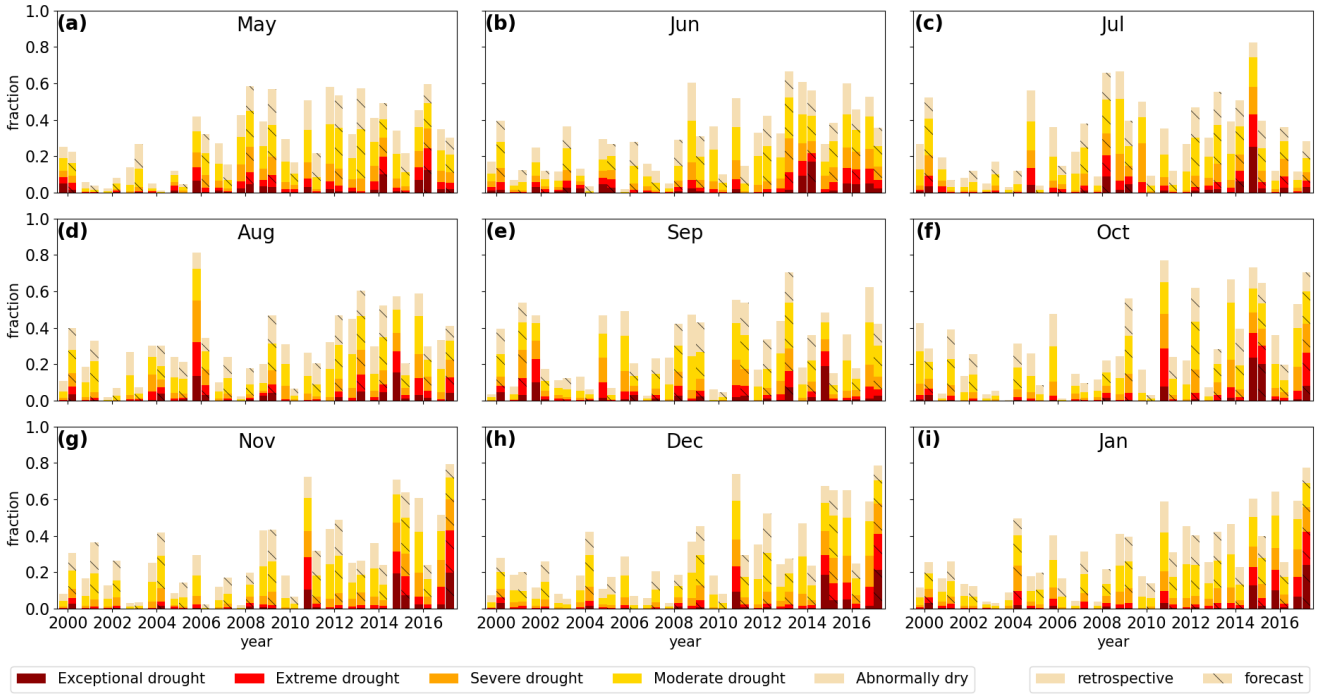

Figure S14: Same as Fig. S13 but for the Brahmaputra basin.

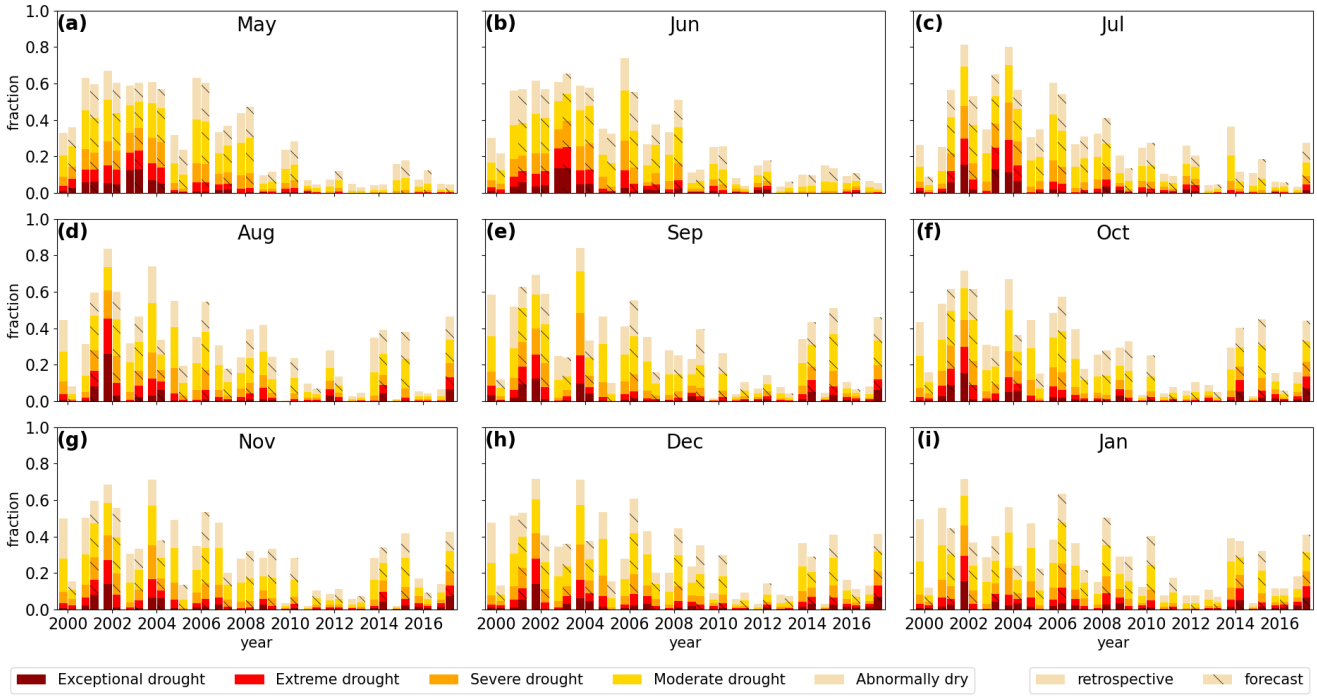

Figure S15: Same as Fig. S13 but for the Indus basin.

85